Histol Histopathol (1995) 10: 289-299

Histology and Histopathology

# Dimorphic myelin in the rat optic nerve as a result of retinal activity blockage by tetrodotoxin during early postnatal period

**D. Crespo, R. Verduga, J. Villegas and C. Fernández-Viadero**
Department of Anatomy and Cell Biology, Faculty of Medicine, University of Cantabria, Santander, Spain

**Summary.** The effects of the retinal ganglion cell (RGC) activity blockage on the early myelination of the rat optic nerve (ON) were investigated at the light and ultrastructural levels. The blockage of the RGC action potential was attained by the use of tetrodotoxin (TTX), a blocker of the voltage-sensitive sodium channels. TTX was either infused directly into the left eye (TON) or injected systematically (SON). These two groups of ONs were compared with the untreated paired right nerves (UON) of the eye-infused group. Our observations showed that the general morphology of the ONs in either treated group was similar to that of the UONs. The most noticeable ultrastructural feature of these nerves was the presence of dimorphic myelin sheaths in 4% of the myelinated fibres (MFs) in the TON group at postnatal day twelve, while they were seldom observed in the other groups (0.5%). These abnormal covers were of two types; long flaps of aberrant myelin or redundant myelin profiles. However, at postnatal day seven, the onset of myelination and the percentage of MFs was similar in the three groups. The morphometric results showed that there were no age-group differences in axon size in unmyelinated and MFs. These results suggest that while the bioelectrical activity of the RGCs could not play any role in maintaining axon calibre it may, to some extent, regulate the process of formation of normal myelin sheaths in the rat ON.

**Key words:** TTX, Optic nerve, Myelin, Rat

## Introduction

Myelin sheaths were described by the microscopists of the last century as compact rings on some nerve fibres (Ranvier, 1878). Cajal (1913), reported the presence in the central nervous system (CNS) of a «third cellular element» apart from neurons and astrocytes, suggesting that it was analogous to the Schwann cells of the peripheral nervous system (PNS). Rio-Hortega (1922), proved that Cajal's third element was indeed a different type of glial cell, and introduced to term oligodendrocyte (OL) to name a cell (cyte) with few (oligo) thick processes (dendro). Later on, Penfield (1924), established the specific role of OLs in the formation of myelin in the CNS. Peters (1960), took up the study of axon myelin formation in the CNS using the optic nerve (ON) as a model and confirmed (Peters and Vaughn, 1967), at the ultrastructural level that OL processes produce great amounts of plasma membrane that enwrap CNS axons forming myelinated fibres (MFs). Oligodendrocytes are small cells with a dark cytoplasm displaying few organelles and bundles of filaments forming the scaffold to cellular processes. These processes may give myelin covers to different axons and/or some regions (internodes) of the same axon. In the PNS each Schwann cell gives origin to only one internode per fibre, while in the CNS an OL may form myelin for several different fibres and/or several internodes of the same fibre. Myelination process involves several steps; the formation of cytoplasmic extensions form the OL; their direct contact with an axonal segment and it being surrounded by the OL elongation membrane. Spirals of this myelin-forming membrane will be added to wrap up the axon. Hence, in any new OL membrane, the cytoplasm is squeezed out to allow myelin-membrane fusion. Mature myelin will be obtained from the compaction of the membrane to form the typical myelin pattern (see Jones and Cowan, 1983). Although formed by two different myelin-forming cells for CNS and PNS, myelin general morphology has been proved to be similar in both locations. The factor(s) that regulate the myelination processes are still a matter of controversy.

In a series of previous papers (Crespo et al., 1985a; O'Leary et al., 1986a; Crespo and Fernández-Viadero,

*Offprint requests to:* Dr. D. Crespo, Departamento de Anatomía y Biología Celular, Facultad de Medicina, Universidad de Cantabria, 39011 Santander, Spain

1989), we have analyzed the fate of rat ON fibres during prenatal and postnatal periods in normal development and under several experiments conditions, such as; eye removal and retinal ganglion cell (RGC) bioelectrical activity blockage. We have now extended our studies in this context to analyze the effects of the blockage of RGC activity on the time course and morphology of the ON fibre myelination. Due to its functional and structural homogeneity the ON constitutes a useful model to correlate morphological and functional studies on a CNS fibre tract. This fact is extended to the analysis of nerve development, since the ON is formed by an entirely unmyelinated tract during the neonatal period. Furthermore, almost all axons become myelinated by the end of the postnatal development (Foster et al., 1982; Crespo et al., 1985). Hildebrand and Waxman (1984), suggested that from a functional point of view the acquisition of a saltatory mode of electrical impulse conduction, as a consequence of the fine myelination process, should be considered as a major developmental stage in the ON. Hence, we have undertaken the study of the relationship between morphological and functional features of the maturing ON by analyzing the myelination process when RGC activity is maintained silent.

The toxicity of Pupper fish poison tetrodotoxin (TTX) has been known since long ago but its exact action mechanism did not become clear until the introduction of voltage clamp procedures (see, Ritchie, 1982). These experiments showed that TTX selective blocks the sodium ion channels that are fundamental to propagate impulses in excitable membranes (Ritchie and Rogart, 1977). In this way we have previously reported (O'Leary et al., 1986a) that blockage of the electrical activity of RGCs by direct eye injections of TTX does not either reduce or delay the normal magnitude and time course of RGC degeneration on the rat. Following this line of investigation we are presenting a study on the effects of TTX on the myelination process pattern and time course during the early postnatal development of the rat ON. A preliminary report of this research has been presented previously in abstract form (Crespo et al., 1992).

## Materials and methods

### *Subjects*

Male rats of the Sprague-Dawley (SD) strain were used. They were bred in our animal facilities and littermates of similar size and weight were selected. Several postnatal ages were employed. The first 24 hours of postnatal life were considered as postnatal day PO (newborn animals), and the ages of the postnatal development analyzed were P3, P7, and P12. During the experimental procedure pups were kept in proper animal cages, mother-nursed, and maintained in a daily 12h light/12h dark cycle. Mothers were fed with chow and received water *ad libitum*.

### *Retinal ganglion cell (RGC) activity blockage*

The animals treated with TTX were the same as those used in previous studies (Crespo et al., 1985b; O'Leary et al., 1986a). They were deeply anaesthetized with ether before RGC activity blocking procedure. The left eyelids were surgically separated from their junctions, due to the fact that in rats they are fused until about P14, when they start to open. Then, the exposed eye (always the left eye) was instilled with a solution of 2% chloranphenicol in 70% alcohol. The sclera was pierced near the ciliar margin with a needle, and through it a micropipette containing a solution of TTX was introduced into the posterior eye chamber as close as possible to the RGC layer. The solution of TTX instilled ranged, depending on animal age, from 0.04 to 0.08 µg (1mg/ml, $3.1x10^{-3}$ in vehicle citrate buffer 0.1M, pH 4.8). As previously reported (O'Leary et al., 1986b) the dose corresponds to roughly half of the lethal amounts for a single dose in every stage. This, it effectively blocks RGC activity which is the relevant point for our purpose. Once the proper amount of solution had been placed into the vitreous, the micropipette was removed, and the eye was again washed with antibiotic solution. When the animals started anaesthetic recovery they were returned to the cage of their mother. In order to keep sustained TTX effect to a maximum, this procedure was performed every other day from PO until perfusion day. It has to be pointed out that due to surgical procedure animal mortality increased notably as the number of injections increased. Thus, for the oldest stage of our study 25% of the starting population died. The same series of animals were injected systematically into the flank with an equivalent age/dose of TTX, as reported previously (Crespo et al., 1985b; O'Leary et al., 1986a).

### *Tissue processing*

After a general anaesthesia the animals were perfused through the heart with saline solution at room temperature to clear out the vascular arbor, followed by a fixative containing 1.5% paraformaldehyde, 3% glutaraldehyde, 0.6% acrolein, 0.6% dimethyl sulphoside (DMSO) and, 3.5% sucrose in 0.1M cacodylate buffer, pH 7.3, at 4 °C. After this, the skull was removed and the posterior part of the exposed brain cut out. This allowed us to tilt down the remaining brain and dissect out the ONs from the optic chiasm to the lamina cribosa. The ONs were rinsed in cacodylate buffer, osmicated in a 2% solution of osmium tetroxide, dehydrated in a series of graded alcohols and embedded in resin. For every age group both the left (TON), and the paired right (UON), and the left ON of the systemic group (SON) were studied. In order to analyze always the same nerve area the embedded ONs were trimmed through their middle point. Semithin transverse sections, 1 µm thick, were cut, mounted onto slides and stained with borated Toluidine blue. These sections were observed with a light microscope under oil immersion

objective to assure no alterations in ON structure. Several TONs, and hence, their UON pairs were discharged due to the fact that RGC damage was presumed. Those reasons were; significative size reduction; and/or the appearance of images suggesting nerves degeneration (O'Leary et al., 1986a). From the selected nerves, ultrathin sections were cut and collected in fomvard-coated single-slot grids, stained with lead citrate (Reynolds, 1963) and examined with a Zeiss EM10 electron microscope at 60 kV.

### *Morphometric analysis*

Electron microscopic photographs of the ONs were employed to measure several ON parameters. This was done with the aid of a digital data tablet (MOP-Videoplan) connected to an image analyzer (Kontron). The percentage of MFs, dimorphic profiles and scrolls in unmyelinated fibres (UFs) were counted. Furthermore, the average diameter of optic axons in UFs and MFs, in every age group was calculated. The usual criteria (Forrester and Peters, 1967; Peters et al., 1991) were applied to differentiate UFs and MFs cut at the node of Ranvier, from other glial processes. The data recorded were statistically processed and compared for significative differences according to ANOVA and a $p<0.05$ was the value for significance.

## Results

### *Light microscopy*

The general morphology of the TONs was undistinguishable from the paired UONs and SONs in all ages. From P3 up to P12 there was an increase in the number of glial, and endothelial cells. At P12, when supporting cells were morphologically more differentiated into OLs and astrocytes, no cellular alterations were evident in any group of animals. In the younger ages, mitotic images indicating proliferation of glial and endothelial cells were frequent. On the opposite side apoptotic bodies suggesting cell degeneration were seldom observed and when present their cellular origin could not be determined. The main observation at P12 was the apparent reduction in the number of MFs in the TONs in comparison to that of the UONs and SONs. Myelinated fibres were considered to be those clearly showing a well-distinguishable myelin ring. Contrary to what can be inferred from the difference in the occurrence of MFs, the start of the process of myelination was not delayed. In all groups the first MFs were clearly visible at P7, and the percentages were similar (see below).

**Table 1.** Percentage of myelinated fibres in the rat ON at two postnatal ages (n=3).

| % MFs/5000 μm² | UON | TON | SON |
|---|---|---|---|
| P7 | 5 | 5 | 5 |
| P12 | 14 | 10* | 14 |

Note that the percentage of MFs is the same at P7 for the three animals groups studied. *: by postnatal day 12, there is a significative difference ($p<0.01$)between UON and SON (14%) in comparison to the value (10%) of MFs for the TONs.

### *Electron microscopy*

At the ages studied, TONs, SONs, and UONs appeared normal in their general ultrastructure as light microscopy suggested. In this period, glial cells were found mainly in a peripheral location in close proximity to the ON surface. Their cytoplasm contained scanty free ribosomes, Golgi complexes, mitochondria and filaments. These cells were astrocytes-like in appearance and formed an array of bodies internally limiting the pial covering of the ON. Apart from this marginal location, there was a less conspicuous distribution of astrocytes on the nerve parenchyma. This last group had long processes which fasciculated the ON parenchyma. It was possible on some occasions, to observe how some of these processes directly contact an axon, but no junctional specialization was present at this level.

### *Myelinated axons (MFs)*

Axons over 0.40 μm in diameter, in all groups, appeared either myelinated or in an advanced process of myelination. Most of the fibre sections corresponded to internodes, and about 2% of sections corresponded to paranodal regions where mesaxons could be clearly seen (Figs. 1-4). As was observed at light microscopic level, the magnitude of MFs was lower in the TONs in comparison to the UONs and SONs (Table 1), but those MFs of the three groups had a similar myelin thickness. In the TON groups the most noticeable morphological fact, was the abundant presence of dimorphic myelin sheaths while they were rarely observed in the other two groups (Table 2). These abnormal myelin profiles can be aberrant myelin profiles, which represented sheaths that after covering an axon extended far away from the ensheatheaning axon following very complicated pathways (Figs. 1-6). The most common morphology of an aberrant myelin profile was an end that contained the

**Table 2.** Percentage of abnormal profiles in myelinated (MFs) and unmyelinated fibres (UFs) of several experimental groups in the rat ON at P12.

| % OF ABNORMAL PROFILES | UON | TON | SON |
|---|---|---|---|
| Dimorphic (MFs) at P7 | - | 1 | 0.5 |
| Dimorphic (MFs) at P12 | 0.5 | 4* | 0.5 |
| Scrolls (UFs) at P7 | 3 | 5** | 3 |
| Scrolls (UMs) at P12 | 5 | 6 | 5 |

Note that percentage of dimorphic profiles, both aberrant and redundant in the TONs is significantly different from that of the UONs, and SONs. *: significative difference, $p<0.001$when compared to UONs and SONs; **: significative difference, $p<0.01$ when compared to UONs and SONs.

axon, and a long, curved flap of myelin that ended in a bulvous formation containing some optic OL cytoplasm (Figs. 1, 5). In some instances both ends contained optic axons (Figs. 2, 6). In our observations three or more axons never appeared ensheathed by the same aberrant myelin cover, through the presence of one of these formations containing three bulbous swellings of glial cytoplasm is reported (Fig. 3). In these loops, myelin membranes appeared separated from each other by the interposition of scanty OL cytoplasm, but at some length

**Fig. 1.** Electron micrograph from the optic nerve of a 12-month-old rat. This nerve corresponds to an eye which was injected with TTX (TON). Some axons have thick compacted myelin sheaths, while most of the axons are still not sheathed. Blood vessels, dark oligodendrocytes, and perivascular astrocytes are present. x 2,000

**Fig. 2.** This image displays the most common configuration of an aberrant myelin profile. It consists of a myelinated fibre in which myelin loses contact with the ensheathed axon and forms an elongation that ends in a bulbous swelling containing some oligodendroglial cytoplasm. In some instances a long flap of aberrant myelin cover trends to fuse, but in most of their length they are separated from each other by the interposition of scanty OL cytoplasm. Rat TON at P12. x 40,000

**Fig. 3.** An aberrant myelin sheath in a TON at P12. One end of this myelin flap contains an axon. To some extent the myelin cover loses contact with the axolemma and after forming the elongation returns to the proceding axon vicinity establishing direct contact between myelin covers. This second end is formed by a bulbous dilation which contains another already myelinated axon, forming a redundant myelin cover. In this particular case both myelin covers are separated by some OL cytoplasm. x 40,000

*Dimorphic myelin*

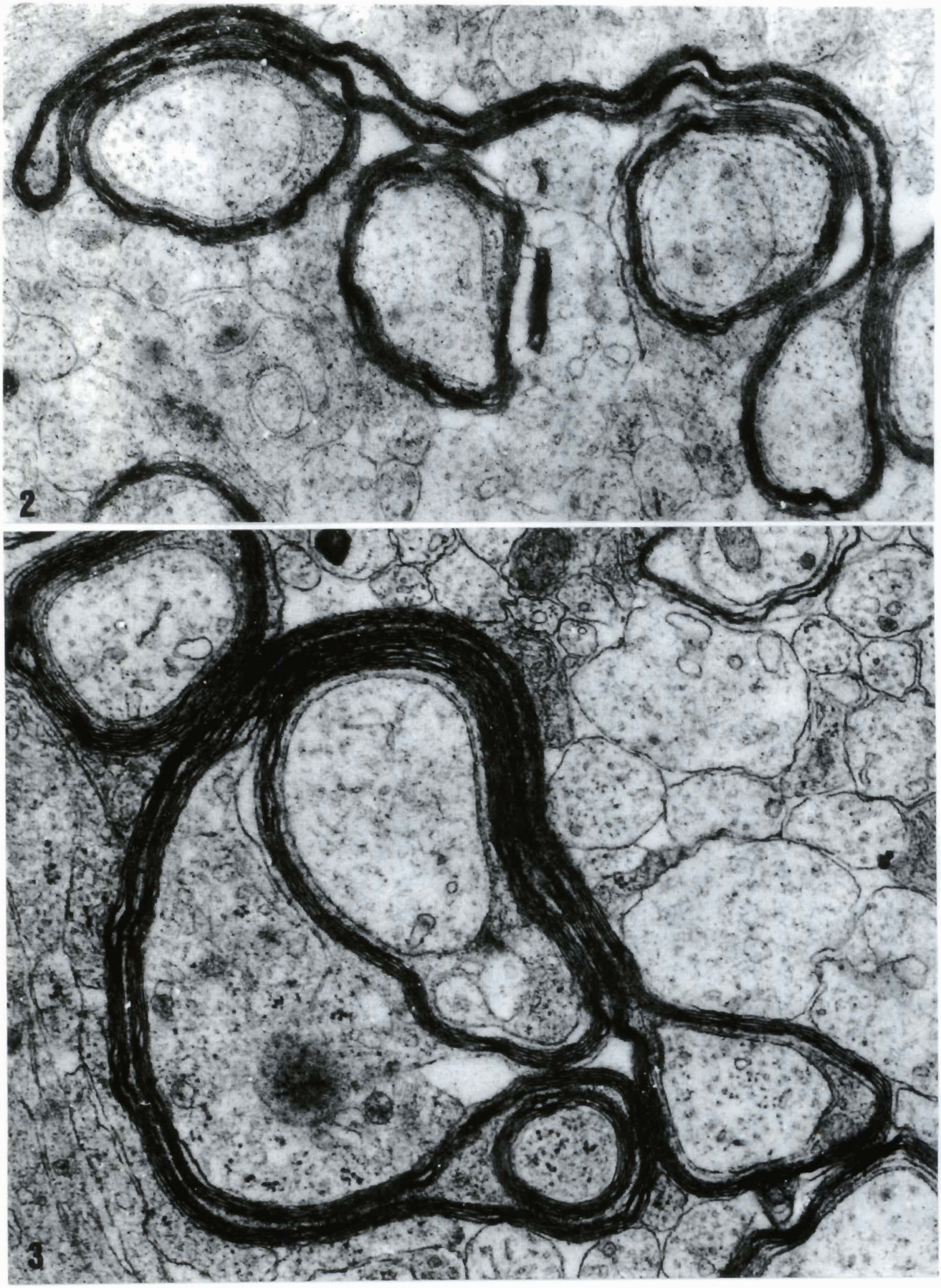


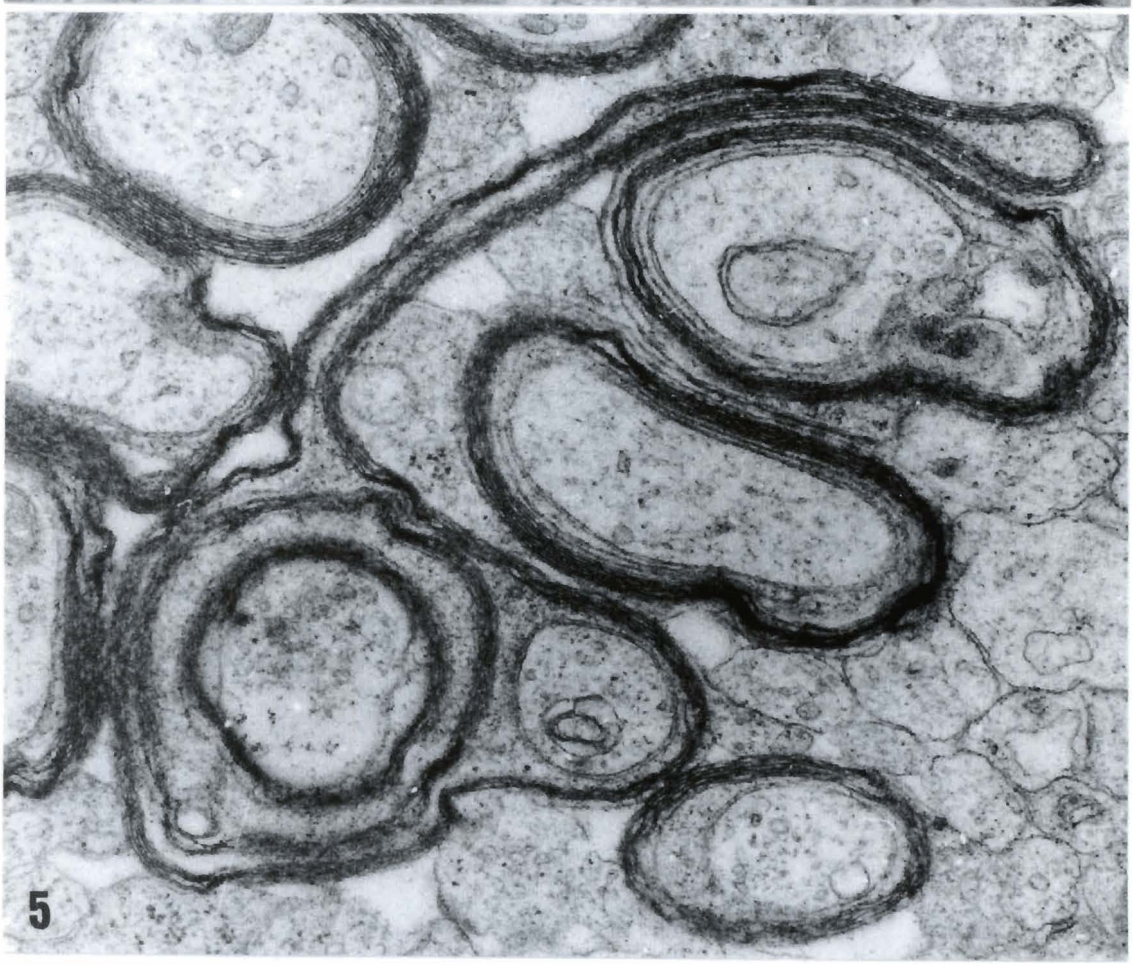


**Fig. 4.** Twelve-day postnatal optic nerve of a TTX-injected eye. This micrograph illustrates an aberrant myelin formation which does not contain any axon. This compacted formation presents three swellings; two of them are found on both ends of this elongation, and the third one occupies roughly the centre of the flap. Observe that these swellings contain some OL cytoplasm. x 40,000

**Fig. 5.** A special type of redundant profile can be observed. An aberrant myelin cover forms a dilation which contains two optic axons. One has three redundant myelin sheaths, and the most external is shared in part with another axon. Observe that all the myelinated axons are of a larger calibre than the unmyelinated ones. P12 TON. x 40,000

the cytoplasm disappeared and myelin covers fused together (Figs. 1-3).

The second type of dimorphic formation was the appearance of a myelin sheath covering an already myelinated axon. Therefore, they formed redundant myelin sheaths (Fig. 2). These redundant covers were separated from each other by glial cytoplasm. Sometimes, the OL cytoplasm disappeared allowing, to some extent, myelin fusion. On some occasions, both types of dimorphic profiles were observed in the same MFs (Fig. 4). In this case, the outermost sheath of a redundant formation covered another axon and formed an extra aberrant myelin lop that ended in a bulbous formation (Fig. 4). Axonal infoldings of myelin sheaths were also observed (Fig. 6). All these dimorphic formations appeared to be constituted by normal myelin in periodicity.

*Unmyelinated fibres (UFs)*

The UFs ran parallel to the ON longitudinal axis, and were coupled to each other to some extent by direct membrane contacts. Apart from their age-related size difference, no morphological variations were observed among groups. UFs contained microtubules, microfilaments and usually mitochondria, which occupied a high proportion of the axon area. On some occasions dilated smooth endoplasmic reticulum cisternae were present. Images of scroll-like membranes appeared in all animal groups, but they were more frequently observed in the early ages. These formations were rounded intraxonal bodies of lamellae that resembled whorls or scrolls of degenerating myelin sheaths (Figs. 5, 6). Scrolls were found intraxonally only in UFs, and were more frequent in the early ages (P3, P7). No periodicity was observed in their membranes and they usually appeared in axons in close proximity to a dimorphic myelin sheath. In these cases the most external lamella established direct contact with the altered myelin profile (Fig. 5).

*Morphometric and quantitative results*

The quantitative results on the percentage of MFs at P7 and P12 appear in Table 1. The most noticeable aspect about the onset of the myelination process was the fact that it occurred by P7, when in all cases studied 5% of the axons were myelinated. From P7 up to P12 there was a remarkable delay in the place of myelination on the TONs. By P12, 14% of the axons in the UON and SON groups were myelinated, while only 10% in the TONs. Moreover, the percentage of dimorphic profiles at P12 was 0.5, 4, and 0.5 for the UONs, TONs, and SONs respectively. On the other hand, the percentage of scrolls at the end of our study was similar in the three groups (Table 2). The morphometric analysis of the nerve fibre sizes reflects the following results; in all P3 groups axon diameter had no significative different. By P7, when the myelination process was evident, the UFs increased their size up to an average of 0.25 μm in calibre for the three groups. Moreover, the myelination process occurred when an axon was over 0.4 μm in width. These morphometric results are summarized in Table 3.

**Table 3.** Axon diameter (μm) at several postnatal ages of myelinated (MFs) and unmyelinated fibres (UFs) of the rat optic nerve in untreated optic nerves (UON), TTX injected (TON), and animals with systemic injections of TTX (SON). Values are mean±SDM, (n=3).

| | | AGE | | | |
|---|---|---|---|---|---|
| | | P0* | P3 | P7 | P12 |
| UON | UFs | 0.17±0.05 | 0.22±0.06 | 0.25±0.05 | 0.30±0.06 |
| | MFs | - | - | 0.52±0.10 | 0.55±0.11 |
| TON | UFs | | 0.21±0.06 | 0.24±0.05 | 0.31±0.05 |
| | MFs | | - | 0.50±0.10 | 0.53±0.09 |
| SON | UFs | | 0.21±0.05 | 0.25±0.05 | 0.29±0.05 |
| | MFs | | - | 0.55±0.10 | 0.55±0.09 |

*: the data on P0 correspond to unpublished values obtained from the analysis of the material of a previous paper (Crespo et al., 1985). See text for more details.

## Discussion

Several strains of rats both control (e.g. Wistar, Long-Evans and, SD), and mutants (e.g. Zitter and, myelin deficient rat) have been employed to study myelination process in the ON. Concomitantly with particular variations in the myelination pattern, morphological alterations in the OLs of some strains have been reported (Kondo et al., 1991; Duncan et al., 1992). In our material, ON glial cells appeared normal in shape and structure in all age groups. During the first postnatal week cell bodies were located in a peripheral position near the ON meningeal cover. Thereafter, glial cells appeared scattered throughout the ON parenchyma. Most of these cells were astrocytes, whereas myelinating OLs were only evident by P7. Thus the more precocious images of early myelination were observed by the end of the first postnatal week. The images of early myelination had the same frequency of appearance (5%) in all groups studied. Moreover, they did not show any preferential location on the ON, being scattered throughout the parenchyma. Thus, this suggests that blockage of the RGC activity neither delays myelination onset nor the distribution of MFs on the TONs. While the ON microvascular system greatly develops during the first postnatal week, as reported previously (Crespo et al., 1989), there was a nearly complete absence of parenchymal and perivascular microglial cells in this same period. Hence, the presence of mitotic endothelial figures was a feature of these early ages. Although the analysis of the percentage of glial cell types was out of the focus of the present study, our observations were in close agreement with Phillips and Krueger (1992), who reported that during the first postnatal week more than 70% of the SD rat ON glial cells were astrocytes.

The most noticeable ultrastructural observation was

*Dimorphic myelin*

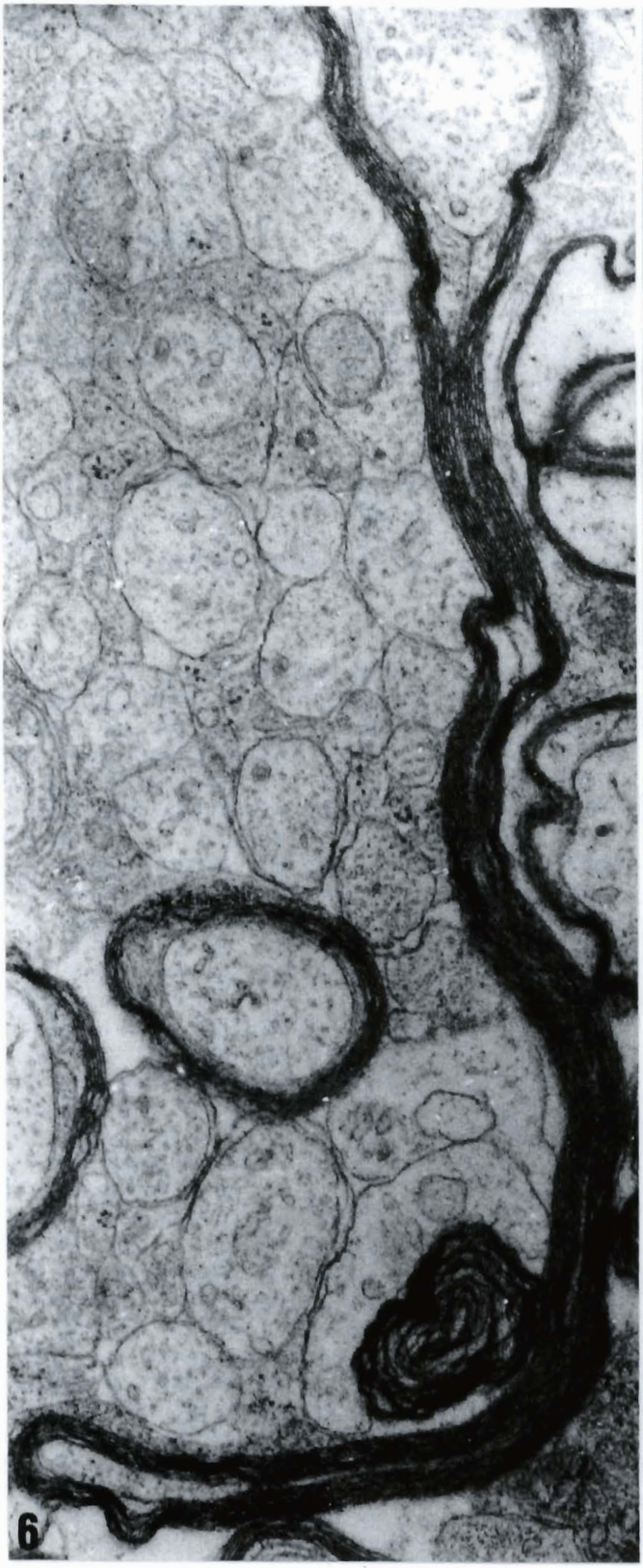


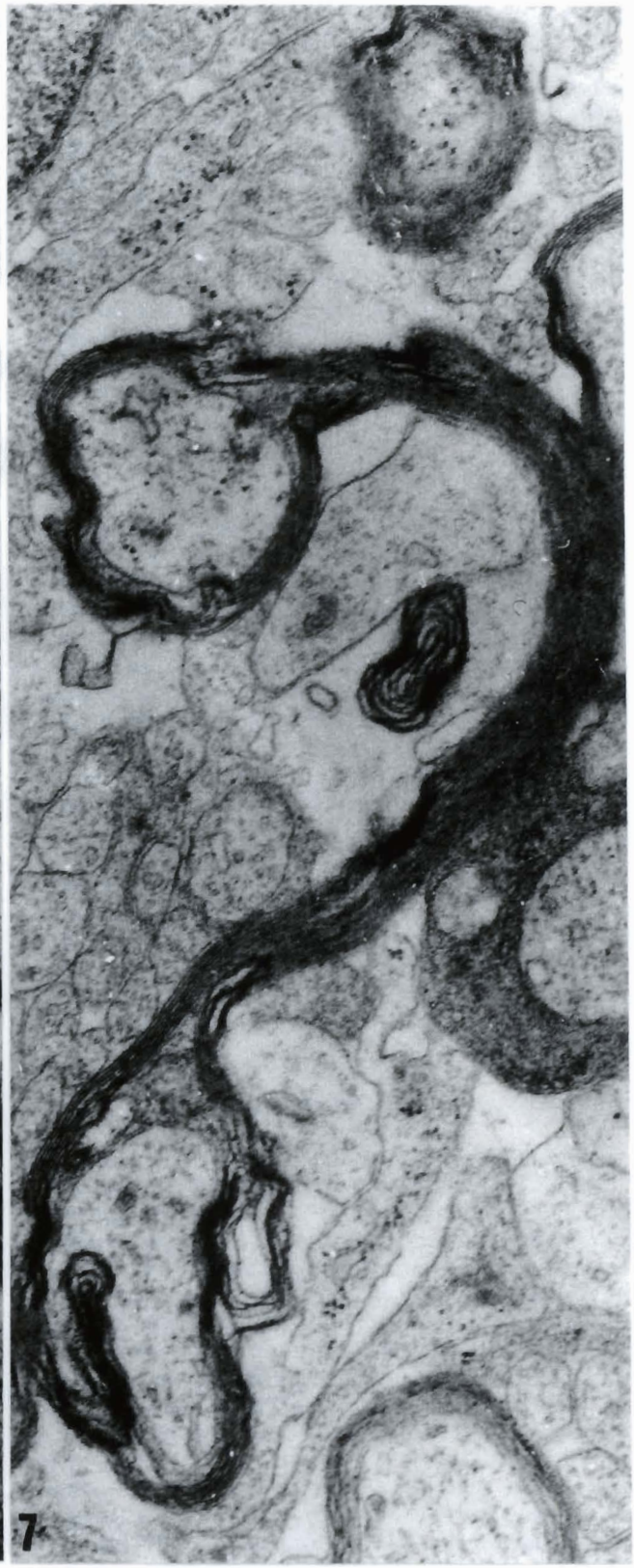

the presence of dimorphic profiles of myelin in the TONs (4%) in comparison to their infrequent observation in the other two groups (0.5%). Thus, the first point to be discussed is whether these alterations might represent a process of RGC damage due to repeated eye injections or if they could be fixation artifacts. Retinal damage has to be discarded since those ONs displaying any degenerative alterations were not included in the study (see Materials and methods). So, at the ultrastructural level, the ONs did not show any morphological sign of induced axonal degeneration. As proposed by Hayat (1981), TTX was instilled in an isotonic vehicle to decrease artifactual alterations in both cells and axons. Furthermore, the perfused solution was an aldehyde mixture well known for preventing fixation artifacts. For myelin stabilization formaldehyde and glutaraldehyde were used to minimize the early degradative changes as a consequence of hypoxia. In the same way the concomitant use of acrolein and DMSO reduces the appearance of myelin alterations (Hayat, 1981). Hence, due to the frequent occurrence of dimorphic myelin profiles in the TONs, whose values are far from exceptions, the alterations reported here have to be related to a modified myelination process.

In the developing ON, the presence of aberrant sheaths had been reported in the zitter rat (Kondo et al., 1991). This strain is an SD mutation which represents an experimental model to analyze hypomyelination. Moreover, the presence of aberrant myelin sheaths in this mutant has been observed in several locations of the CNS (Kondo et al., 1992). Those abnormal sheaths in the zitter ON had very important differences with the aberrant covers of our material. In the mutant, myelin profiles did not contain axons, so they were formed by myelin covers fused together in all their length. Thus, neither lumen non areas of oligodendroglial cytoplasm were present. When studying the ONs of SD and Wistar rats on the appearance of aberrant profiles, Kondo et al. (1992) reported that they were not observed in any of these strains from P0 up to P12. Hence, this suggests that the possibility of aberrant profiles being strain-dependent has to be excluded. Another characteristic which made zitter aberrant covers different from the ones of the SD rat observed here was the time of appearance. In our material they came into view as early as P7 when myelination started while in the zitter rat their arousal was deferred until the end of the second postnatal week. To the best of our knowledge no study has been performed either on the activity or the postnatal elimination of zitter RGCs. Hence, the alterations reported in this mutant could be the morphological expression of an altered bioelectrical transmission activity. Furthermore, the concomitant action in this mutant of a morphogenetic variation with an altered bioelectrical activity cannot be excluded either. If so, this would support our observations on the increased presence of dimorphic myelin profiles referring to blockage of the RGCs bioelectrical activity.

In the PNS, aberrant myelin covers had been reported in the sciatic nerve (SN) of controls and animals under several experimental conditions. In the rat SN, Peters and Vaughn (1967), reported the presence of aberrant myelin. These SN flaps consisted of an axon in which myelin cover loses contact, to some extent, with the axolemma, forming a single myelin profile. These flaps, as intracytoplasmic Schwann cell formations, were short in length. Moreover, they cannot form redundant myelin sheaths on another fibre as is the case of the ON. These characteristics made SN myelin flaps different from the aberrant myelin profiles of the blocked ON. In the adult guinea pig SN, Webster et al. (1961) reported aberrant profiles of myelin. There, the paranodal portion of myelin sheaths exhibited flaps in a similar fashion to the ones of the rat ON. These guinea pig SN flaps appeared in approximately 75% of the largest MFs, a percentage that is a higher value than the one at the end of our study. In this sense we found 4% of dimorphic covers when only 10% of the axons were myelinated on the TONs. This indicates that the total hypothetic value of dimorphic profiles for a full myelinated TTX blocked ON will correspond to roughly 30% of the total number of ON fibres.

The presence of redundant covers in the CNS has been reported by several authors. Rosenbluth (1966), reported the presence of abundant dimorphic myelin sheaths in the cerebellum of the toad. These sheaths after losing contact with their surrounding axon, tended to enroll other MFs, forming similar configurations to the redundant figures of the ON. In our material, redundant formations were never observed covering any glial cell body, but in the case of the toad cerebellum, they enwrapped granule cell bodies, dendritic segments, and were also observed covering glial processes. In another CNS location, the inferior oliva of the cat, Walberg (1964), had already reported the presence of several axons surrounded by a common myelin sheath. Based upon close axolemma contacts among the fibres enwrapped by these redundant covers, he suggested that they represented regions of axonal branching. In the case of the rat ON, we believe that redundant myelin sheaths are not formed due to fibre division, based on the following considerations: first, no axonal branching has been reported in the rat ONs, and the number of axons remains constant along the ON length (Lia et al., 1986);

**Fig. 6.** In this micrograph an aberrant myelin profile wraps an unmyelinated axon which contains a scroll-like formation. Observe that the membranes that form this lamellar body do not show the ultrastructural pattern of the aberrant myelin of the vicinity. Note that there is a close relationship between these two formations. Optic nerve TTX-infused. P12. x 40,000

**Fig. 7.** Dimorphic myelin figure which contains two axons at each end. Note that the axon found on the lower part contains a myelin infolding. A scroll-like formation, with no direct relation to any type of fibre is observed here. Postnatal day 12. TON. x 40,000

secondly, in the same cross-section area, redundant sheaths covered axons that were located too far apart from each other to support the fact that they may appear on axonal divisions, as was suggested by Walberg (1964) for the inferior oliva of the cat.

From a quantitative point of view, the most conspicuous observation affecting axonal morphology was the presence of scrolls of membranes only in the UFs of the three groups of ONs. Hildebrand and Waxman (1984) reported similar membranous inclusions during the early development of the ON of the Long-Evans (LE) rat. Those bodies, as the ones observed here, were composed of loosely-packed concentric lamellae. They occurred on about 2-4% of the population of UFs of the LE rat, while our observations establishes this value in 5-6% for the SD rat. Remahl and Hildebrand (1990), found scrolls in the developing spinal cord and corpus callosum of the cat. These scrolls were composed of two to ten layers of loosely-arranged membranes of similar morphology and shape to the ones present in the rat ONs. As in the case of the LE rat, they appeared only in UFs just prior to the start of ensheathment. After SN transection in adult rats, various types of ultrastructural degenerative changes in the gracile nucleus (GN) have been observed (Persson et al., 1991). Apart from the induced SN injury the occurrence in the GN of large myelinated profiles containing intraxonal lamellar formations was reported. These formations were similar to the ones of the ON, but with a more developed morphology. It was suggested that these scrolls in the CNS were the morphological expression of a process of exocytosis before onset of myelination (Hildebrand and Waxman, 1984), while in the PNS it was proposed that they were the morphological expression of an advanced degradation level of intraxonal organells (Persson et al., 1991). This last proposal is in accordance with our previous observation on the elimination of up to 75% of the axons initially generated to form the adult rat ON (Crespo et al., 1985a,b). In fact some of these lamellar bodies have been observed free on the ON parenchyma with no relationship with any other ON structure, suggesting that they may well represent axon remnants in an advanced degenerative process.

The postnatal development of the ON represents a period where, concomitantly with axon and glial maturation, there are significative functional processes taking place, such as: initialization of electric impulse transmission (Hildebrand and Waxman, 1984). In this context, several studies have proven that glial development in the ON is a complex process (Miller et al., 1989). During the first postnatal week of the rat, precursor glial cells divide to generate type-1 astrocytes and O-2A progenitor cells. These O-2A, in turn, proliferative to form mature astrocytes (type-2) and OLs, resulting in a new distribution of the ion channel of optic axon repertoire (Ritchie, 1982; Raff, 1989; Fulton et al., 1991; Kettenmann et al., 1991). This general rearrangement in the ON ion channels has been proposed to reflect the functional transition to a more differentiated state (Fulton et al., 1991). The fact that this functional maturation is taking place in close relationship with the process of myelination, may well suggest that ion channel function could be related, to some extent, to a process of information exchange between the axolemma and the premyelinating OL. In summary, the results of the present study demonstrate the frequent occurrence of dimorphic ultrastructural myelin profiles under direct RGC exposure to TTX, while altered covers were seldom observed in UONs and SONs. Since the possibility that these alterations in myelin spatial configuration could represent either fixative artifacts or be the result of RGC damage were discarded, we conclude that our observations suggest that the maintenance of a normal bioelectrical activity plays some role in the regulation of myelin shape in the ON of the rat.

*Acknowledgements.* This study was initiated when D. Crespo was a Fogarty International Center Fellow visiting the Salk Institute. The sponsorship of W.M. Cowan and the teaching of D.D.M. O´Leary are deeply acknowledged. The authors wish to thank Mr. J. Rokos and Mrs. R. Garcia for performing excellent technical assistance. The work in our laboratory has been supported by Grant PM91-0170 from DGICYT.

## References

Cajal S.R. (1913). Contribución al conocimiento de la neuroglía del cerebro humano. Trab. Lab. Invest. Biol. Univ. Madrid. 11, 255-315.

Crespo D. and Fernández-Viadero C. (1989). The microvascular system of the optic nerve in control and enucleated rats. Microvasc. Res. 28, 237-242.

Crespo D., O'Leary D.D.M. and Cowan W.M. (1985a). Changes in the number of optic nerve axons during late prenatal and early postnatal development of the albino rat. Dev. Brain Res. 19, 129-134.

Crespo D., O'Leary D.D.M., Fawcett J.W. and Cowan W.M. (1985b). Minimal effect of intraocular tetrodotoxin on the postnatal reduction in the number of optic nerve axons in the albino rat. Soc. Neur. Abstr. 11, 259.

Crespo D., Fernández-Viadero D. and Villegas J. (1992). Redundant myelin sheaths in tetrodotoxin treated rat optic nerves. Eur. J. Neurosci. 5S, 31.

Duncan I.D., Lunn K.F., Holmgren B., Urba-Holmgren R. and Brigno-Holmes L. (1992). The taiep rat: A myelin mutant with an associated oligodendrocyte microtubular defect. J. Neurocytol. 21, 870-884.

Forrester J. and Peters A. (1967). Nerve fibers in optic nerve of rat. Nature 241,2 45-247.

Foster R.E., Connors B.W. and Waxmann S.G. (1982). Rat optic nerve: electrophysiological, pharmacological and anatomical studies during development. Dev. Brain Res. 3, 371-386.

Fulton B.P., Burne J.F. and Raff M.C. (1991). Glial cells in the rat optic nerve: the search for the type-2 astrocyte. In: Glial-neuronal interaction. Abbott N.J. (ed). Ann. N.Y. Acad. Sci. New York. vol. 633, pp 27-34.

Hayat M.A. (1981). Fixation for electron microscopy. Academic Press. New York. pp 90-245.

Hildebrand C. and Waxmann S.G. (1984). Postnatal differentiation of rat optic nerve fibres: electron microscopic observations on the

development of nodes of Ranvier and axoglial relations. J. Comp. Neurol. 224, 25-37.

Jones E.G. and Cowan W.M. (1983). The nervous tissue. In: The structural basis of neurobiology. Jones E.G. (ed). Elsevier. New York. pp 283-351.

Kettenmann H., Blankenfeld G.V. and Trotter J. (1991). Physiological properties of oligodendrocytes during development. In: Glial neuronal interaction. Abbott N.J. (ed). Ann. N.Y. Acad. Sci. New York. vol. 633. pp 64-77.

Kondo A., Sata Y. and Nagara H. (1991). An ultrastructural study of oligodendrocytes in zitter rat: A new animal model for hypomyelination in the CNS. J. Neurocytol. 20, 929-936.

Kondo A., Sendoh S., Akazawa K., Sato Y. and Nagara H. (1992). Early myelination in zitter rat: morphological, immunocytochemical and morphometric studies. Dev. Brain Res. 67, 217-228.

Lia B., Williams R.W. and Chalupa L.M. (1986). Does axonal branching contribute to the overproduction of optic nerve fibers during early development of the cat's visual system? Dev. Brain Res. 25, 296-301.

Miller R.H., French-Constant C. and Raff M.C. (1989). The macroglial cells of the rat optic nerve. Ann. Rev. Neurosci. 12, 517-534.

O'Leary D.D.M., Crespo D., Fawcett J.W. and Cowan W.M. (1986a). The effect of intraocular tetrodotoxin on the postnatal reduction in the numbers of optic nerve axons in the rat. Dev. Brain Res. 30, 96-103.

O'Leary D.D.M., Fawcett J.W. and Cowan W.M. (1986b). Topographic targeting errors in the retinocollicular projection and their elimination by selective ganglion cell death. J. Neurosci. 12, 3692-3705.

Penfield W. (1924). Oligodendroglia and its relation to classical neuroglia. Brain 47, 430-452.

Persson J.K.E., Aldskogius H., Arvidsson J. and Homberg A. (1991). Ultrastructural changes in the gracile nucleus of the rat after sciatic nerve transection. Anat. Embryol. 184, 591-604.

Peters A. (1960). The formation and structure of myelin sheaths in the central nervous system. J. Biophys. Biochem. Cytol. 8, 431-446.

Peters A. and Vaughn J.E. (1967). Microtubules and filaments in the axons and astrocytes of early postnatal rat optic nerves. J. Cell Biol. 32, 113-119.

Peters A., Palay S.L. and Webster H. de F. (1991). The fine structure of the nervous system: The neurons and supporting cells. Oxford Univ. Press. Oxford. pp 89-120.

Phillips D.E. and Krueger S.K. (1992). Effects of combined pre- and postnatal ethanol pressure (three trimester equivalency) on glial cell development in rat optic nerve. Int. J. Dev. Neurosci. 3, 197-296.

Raff M.C. (1989). Glial cell diversification in the rat optic nerve. Science 243, 1450-1455.

Ranvier L. (1878). Leçons sur l'histologie du système nerveux. F. Savy. Paris.

Remahl S. and Hildebrand C. (1990). Relations between axons and oligodendroglial cells during initial myelination. II. The individual axons. J. Neurocytol. 19, 883-889.

Reynolds E.S. (1963). The use of lead citrate at high pH as an electron opaque stain in electron microscopy. J. Cell Biol. 17, 208-217.

Rio-Hortega P. (1922). ¿Son homologables la glía de escasas radiaciones y la célula de Schwann? Bol. Soc. Esp. Biol., 10, 25-45.

Ritchie J.M. (1982). Distribution and functional significance of sodium and potassium channels in normal and acutely demyelinated mammalian myelinated nerve. In: Neuronal-glial cell interrelationships. Sears T.A. (ed). Springer-Verlag. New York. pp 251-269.

Ritchie J.M. and Rogart R.B. (1977). The binding of saxitonin and tetrodotoxin to excitable tissue. Rev. Physiol. Biochem. Pharmacol. 79, 1-50.

Rosenbluth J. (1966). Redundant myelin and other structural features of the toad cerebellum. J. Cell Biol. 28, 73-93.

Walberg F. (1964). Further electron microscopical investigation of the inferior olive of the cat. In: Progress in brain research. Topics in basic neurology. Bragmann W. and Schade J.P. (eds). Elsevier. Amsterdam. pp 59-75.

Webster H. de F., Spiro D., Waksman B. and Adams R.D. (1961). Schwann cell changes in guinea pig sciatic nerves during experimental diphteritic neuritis. J. Neuropathol. Exp. Neurol. 20, 5-34.

Accepted November 7, 1994